

Constraints on the gas fraction from *ROSAT* PSPC observations of high-luminosity clusters of galaxies

S. Ettori and A.C. Fabian

Institute of Astronomy, Madingley Road, CB3 0HA Cambridge, England

ABSTRACT

We present a detailed and homogeneous analysis of the *ROSAT* PSPC surface brightness profiles of 36 clusters of galaxies with high X-ray luminosity ($L_X > 10^{45}$ erg s $^{-1}$) and redshifts between 0.05 and 0.44. Using recent *ASCA* estimates of the temperature of the gas for most of the clusters in the sample, we apply to the surface brightness profiles (i) the deprojection technique and (ii) the fit with both the β -model and an analytic gas profile obtained under the assumption that the gas is isothermal and in hydrostatic equilibrium with Navarro-Frenk-White dark matter potential [$\rho_{\text{gas}} = \rho_0(1+x)^{\eta/x}$].

This allows us to describe the gas and dark matter distributions in high X-ray luminosity clusters to constrain their gas mass fraction estimate.

1. Introduction

The physics of the formation of clusters of galaxies depends upon the cosmological parameters, $\Omega_{0,m}$ and Ω_b , that measure the total matter density and the baryon density with respect to the critical value, ρ_c , respectively. Assuming that clusters of galaxies retain the same ratio $\Omega_b/\Omega_{0,m}$ as the rest of the Universe, a direct constraint on $\Omega_{0,m}$ is given by comparing the cluster baryon fraction with Ω_b , which is estimated from the agreement between the predicted and observed abundances of the light elements (i.e. D, ^3He , ^4He , ^7Li) within the standard primordial nucleosynthesis theory (see, f.ex., Hogan 1997).

In the X-ray waveband, where most of the baryons are observable, the information on the gas and total mass distributions is inferred from spectral and spatial analyses. To properly know the gas density, we need to deproject the observed surface brightness profile, which is simply the projection on the sky of the (mostly) bremsstrahlung emissivity. To constrain the total mass, we make use of the hydrostatic equation with a temperature profile that we assume isothermal (but see Sect. 2). In particular, we are interested in the temperature of the bulk of the cluster gas, possibly not affected from the presence of any cooling central gas, which can lead to a lower (emission-weighted) temperature. Thus, in the following analysis, we consider gas temperatures that have been measured either excluding the core region (Markevitch et al. 1998) or including a cooling flow component in the spectral fit (Allen & Fabian 1998).

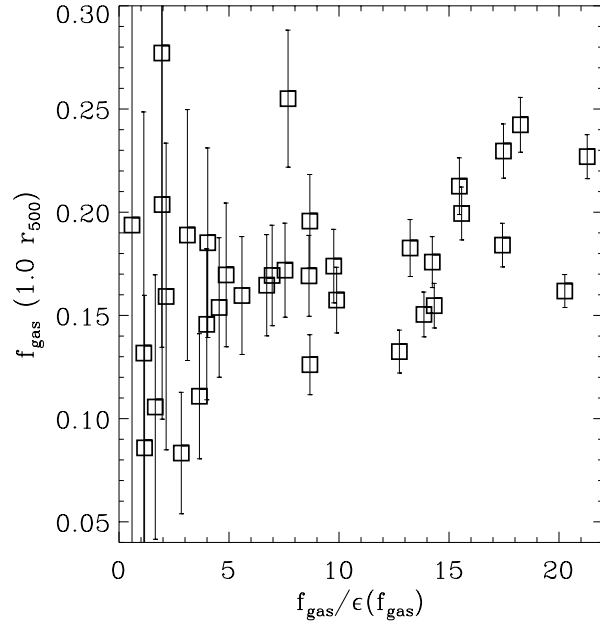


Fig. 1.— The gas mass fraction values for our 36 clusters are plotted versus the ratio $f_{\text{gas}}/\epsilon(f_{\text{gas}})$. Only the 30 clusters with $f_{\text{gas}}/\epsilon(f_{\text{gas}}) > 2$ have been considered in our final sample.

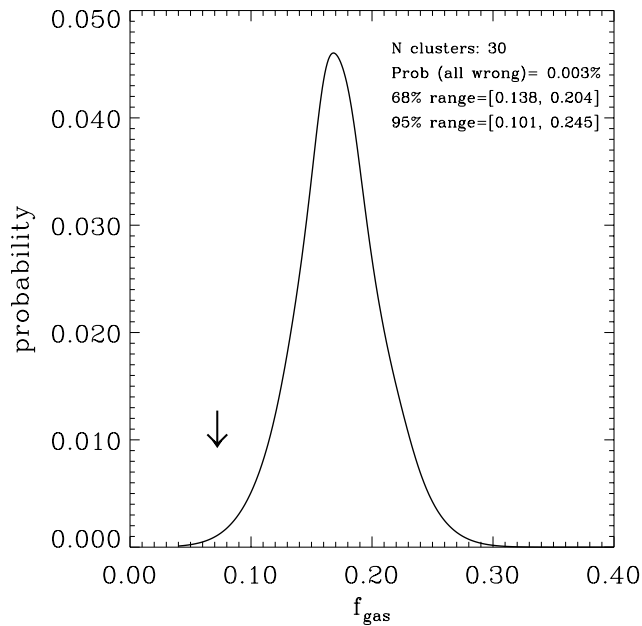


Fig. 2.— Bayesian probability distribution for the gas fraction observed in the clusters in our refined sample of 30 clusters. This distribution peaks at $f_{\text{gas}} = 0.168$. The arrow indicates the constraints from the primordial nucleosynthesis value for the low D/H case (e.g. Hogan 1997). It has a probability of 7.2×10^{-3} with respect to the plotted distribution when an Einstein-de Sitter Universe is considered with $H_0 = 50 \text{ km s}^{-1} \text{ Mpc}^{-1}$.

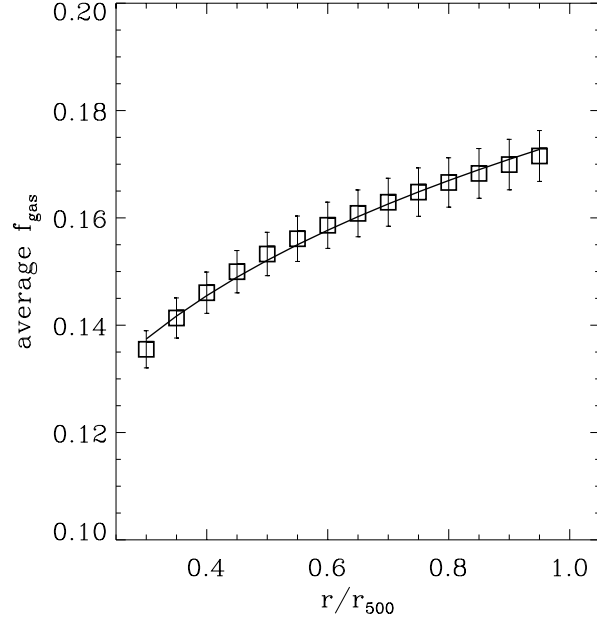


Fig. 3.— The average (with the respective error) of f_{gas} from the 30 clusters in our sample is here plotted at different radii (r_{500} is the radius where the overdensity of the dark matter with respect to the average value is 500). We overplot the best-fit power law with index of 0.20 ± 0.02 .

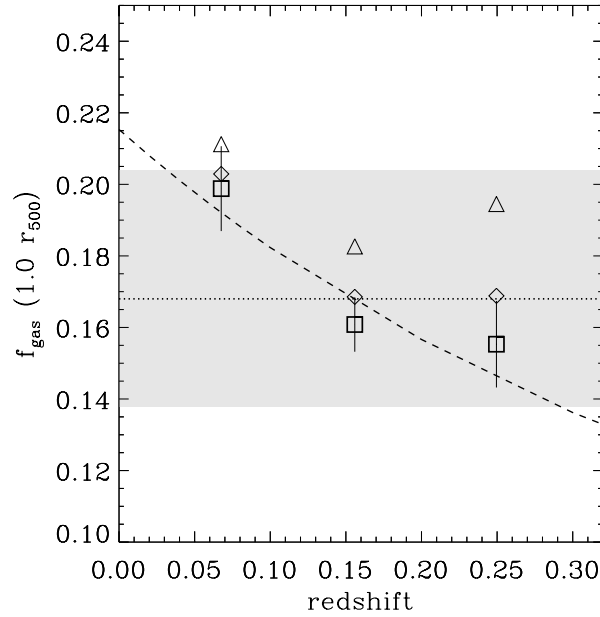


Fig. 4.— f_{gas} **vs redshift**. The best-fit result is $0.215(-0.019, +0.020) (1+z)^{-1.75(-0.65, +0.65)}$. When a different cosmology is considered into the dependence of f_{gas} upon $d_{\text{ang}}^{1.5}$, we obtain the values represented with *diamond* ($\Omega_{0,m} = 0.2, \Omega_{\Lambda} = 0$) and *triangle* ($\Omega_{0,m} = 0.2, \Omega_{\Lambda} = 1 - \Omega_{0,m}$). The shaded region shows the 1σ -scatter range of f_{gas} (the dotted line represents the central value) from the robust analysis on 30 clusters.

Table 1: The 36 clusters in our sample with ROSAT *PSPC* archive observations. The gas temperature are collected from literature (we consider, when available, the values measured excluding the cooling flow regions in the spectral analysis). The profiles extracted to R_{out} (h_{50}^{-1} Mpc) are then both deprojected and fitted to constrain the gas and total masses.

cluster	z	α_{2000}	δ_{2000}	T_{gas} (keV)	R_{out}
A401	0.0748	02 ^h 58 ^m 56 ^s .1	+13° 34' 55''	8.0 ± 0.2	2.10
A478	0.0881	04 13 23.9	+10 28 04	8.1 ± 0.7	2.05
A483	0.2800	04 15 54.8	−11 32 17	8.7 ± 2.0	1.19
A520	0.2030	04 54 08.2	+02 55 42	8.3 ± 0.5	1.86
A545	0.1530	05 32 24.0	−11 32 15	5.5 ± 6.2	2.34
A586	0.1710	07 32 18.6	+31 38 19	10.7 ± 6.3	1.19
A644	0.0704	08 17 24.5	−07 30 29	8.1 ± 0.5	3.02
A665	0.1816	08 30 56.3	+65 50 52	9.0 ± 0.4	2.24
A1068	0.1386	10 40 42.6	+39 57 22	5.5 ± 0.9	1.20
A1413	0.1427	11 55 17.6	+23 24 28	8.5 ± 0.8	1.53
A1651	0.0825	12 59 20.6	−04 11 30	6.1 ± 0.2	2.91
A1689	0.1810	13 11 28.7	−01 20 17	10.0 ± 0.7	1.59
A1763	0.1870	13 35 17.0	+41 00 07	9.7 ± 0.4	2.05
A1795	0.0621	13 48 51.3	+26 35 46	5.9 ± 0.2	1.49
A1835	0.2523	14 01 00.9	+02 53 10	9.8 ± 1.4	1.41
A2029	0.0765	15 10 54.7	+05 45 07	8.5 ± 0.2	2.17
A2142	0.0899	15 58 18.3	+27 14 07	9.3 ± 0.8	2.49
A2163	0.2030	16 15 44.6	−06 08 45	13.8 ± 0.5	2.37
A2204	0.1523	16 32 46.1	+05 34 55	9.2 ± 1.5	1.50
A2218	0.1750	16 35 49.3	+66 12 58	7.1 ± 0.2	2.01
A2219	0.2280	16 40 17.5	+46 42 58	12.4 ± 0.5	2.29
A2244	0.0970	17 02 40.2	+34 03 37	7.1 ± 2.4	1.40
A2256	0.0581	17 03 08.1	+78 39 19	7.1 ± 0.2	2.50
A2319	0.0559	19 21 09.9	+43 56 58	9.3 ± 0.2	2.61
A2390	0.2279	21 53 35.1	+17 42 06	11.1 ± 1.0	2.01
A2507	0.1960	22 56 49.8	+05 30 28	9.4 ± 1.6	1.69
A2744	0.3080	00 14 17.5	−30 23 32	11.0 ± 0.5	1.42
A3112	0.0746	03 17 55.6	−44 13 56	4.1 ± 1.4	1.35
A3266	0.0594	04 31 15.9	−61 26 48	8.0 ± 0.3	2.04
A3888	0.1680	22 34 26.3	−37 43 50	9.0 ± 1.2	1.28
IRAS 09104	0.4420	09 13 45.2	+40 56 31	8.5 ± 3.4	1.42
MS 1358	0.3290	13 59 49.4	+62 31 19	7.5 ± 4.3	1.22
MS 2137	0.3130	21 40 13.9	−23 39 29	5.2 ± 1.1	1.10
PKS 0745	0.1028	07 47 30.1	−19 17 09	8.7 ± 1.0	1.93
Triang. Aus.	0.0510	16 38 20.4	−64 21 14	10.1 ± 0.7	2.41
Zw 3146	0.2906	10 23 39.3	+04 11 31	11.3 ± 3.5	1.05

2. Two or three things about f_{gas}

We select from our sample the 30 clusters where the value of $f_{\text{gas}}(< r_{500})$ is twice its uncertainty, i.e. we apply the selection criterion that $f_{\text{gas}}/\epsilon(f_{\text{gas}}) > 2$ (**Fig. 1**).

We show in Fig. 2-4 some results of our study on the cluster gas fraction more widely discussed in a forthcoming paper (Ettori & Fabian 1998). We present in Sect. 3 our main conclusions.

In this Section, we consider the dependence of f_{gas} on the gas temperature profile. Markevitch

et al. (1998) claim, from the analysis of a sample of clusters observed from *ASCA*, that a negative temperature gradient is generally present and well represented by a polytropic function with index, γ , of 1.2-1.3 between 1 and 6 X-ray core radii. They have assumed a β -model for the gas density with $[\beta, r_c]$ of [0.67, 0.3 Mpc].

The total mass is then corrected of about 1.2 – 0.6 over the radial range $[1, 6]r_c$. It yields a larger gas fraction with respect to the isothermal case, above 2 r_c . At $r \sim 6 r_c \sim r_{500}$, $f_{\text{gas}}^{\text{polytropic}}$ can be larger than $f_{\text{gas}}^{\text{isothermal}}$ by a factor of 1.6.

For a gas still in hydrostatic equilibrium with the Navarro-Frenk-White (1995) potential but described by a polytropic equation of state, we obtain the following temperature profile:

$$\frac{T_{\text{gas}}(r)}{T_0} = 1 + \eta \frac{\gamma - 1}{\gamma} \left[\frac{\ln(1 + x)}{x} - 1 \right], \quad (1)$$

where $T_0 = T_{\text{gas}}(0)$, $x = r/r_s$ and $\eta = \frac{4\pi G \rho_s r_s^2 \mu m_p}{k T_0}$ (see Ettori & Fabian 1998 for details). We have fitted the polytropic gas equation to the profiles of the clusters with enough data points. Although the distribution of the best-fit results provides $\gamma = 1.25 \pm 0.13$, the F-test shows that none of these polytropic fits is better than the isothermal one at 95% c.l.

We note that steep electron temperature profiles need not be representative of the state of the gas if the Coulomb collisions between ions and electrons are in-efficient (see, for ex., Ettori and Fabian 1997). When the equipartition time is comparable to the age of the last, large merger, the mean gas temperature is then generally flatter than the X-ray observed electron temperature profile.

3. SUMMARY AND CONCLUSIONS

In the refined sample of 30 hot (median $T_{\text{gas}} = 9$ keV) and intermediate distance (median $z = 0.1680$) clusters of galaxies, we have applied both the deprojection technique and the fitting approach obtaining the same values of f_{gas} within a median deviation of less than 1σ . We measure a median best-fit $[\beta, r_c] = [0.71, 0.24$ Mpc] for the β -model, and $[\eta, r_s] = [10.20, 0.75$ Mpc] for the gas profile, $\rho_{\text{gas}} = \rho_0(1 + x)^{\eta/x}$. A linear relation is also found between $r_c - r_s$ and $\beta - \eta$.

About the gas fraction, f_{gas} , we observe that:

1. $f_{\text{gas}}(r_{500})$ values have a biweight location and scale of 0.171 ± 0.035 . When Bayesian statistics is adopted, the probability distribution is peaked at 0.168 and has a 95 per cent range of [0.101, 0.245] (**Fig. 2**). With respect to this distribution, the highest estimate of Ω_b (corresponding to a low deuterium abundance) has a probability of 7.2×10^{-3} in an Einstein-de Sitter Universe. If we consider the cosmological correction in the angular size–redshift relation for a flat Universe with $\Omega_\Lambda = 0.8$, we measure a biweight value (with bootstrap error) of $0.196(\pm 0.006)$.

2. Many of the individual estimates of f_{gas} are inconsistent with the average value or with each other, confirming that there are real differences in the measured gas fractions in clusters.
3. The average dependence upon the radius within a cluster is r^s , with $s \sim 0.20$ (**Fig. 3**). In general, we can write $f_{\text{gas}} \propto r^{-2.2-s_{\text{DM}}}$, where s_{DM} is the slope of the dark matter profile.
4. In our sample of high-luminosity clusters, there is a significant correlation between f_{gas} and redshift as $f_{\text{gas}}(r_{500}) \propto (1+z)^{-1.75(\pm 0.65)}$. When we take it into account, there is then only a mildly significant dependence of $f_{\text{gas}}(r_{500})$ upon the temperature (and, even weaker, upon the mass). The dependence upon redshift weakens in a low matter density universe, in particular if a cosmological constant is present (**Fig. 4**).
5. Adopting a low abundance for deuterium (i.e. a high Ω_b), $H_0 = 73 \pm 14 \text{ km s}^{-1} \text{ Mpc}^{-1}$ (Freedman et al. 1998) and requiring that any physical source in redistributing the energy within the cluster cannot produce large variations in the value of f_{gas} quoted above, we constrain at 95% confidence level

$$\Omega_{0,m} < \frac{\Omega_b}{f_{\text{gas}}} \left(\frac{H_0}{50 \text{ km s}^{-1} \text{ Mpc}^{-1}} \right)^{-0.5} < 0.56 \text{ (0.33, with the highest estimate of } f_{\text{gas}})$$

6. Future X-ray missions, and **XMM** in particular, can constrain better the temperature gradient in the electron (and electron+ion) population in the outer cluster regions. If the indication of a negative gradient in T_{gas} is confirmed, f_{gas} can rise (and $\Omega_{0,m}$ drop) by a factor of 1.6.

REFERENCES

- Allen S.W. & Fabian A.C., 1998, MNRAS, 297, L57
- Ettori S. & Fabian A.C., 1997, MNRAS, 292, L33
- Ettori S. & Fabian A.C., 1998, MNRAS, submitted
- Freedman W.L., Mould J.R., Kennicutt Jr R.C. & Madore B.F., 1998, astro-ph/9801080
- Hogan C.J., 1997, astro-ph/9712031
- Markevitch M., Forman W.R., Sarazin C.L. & Vikhlinin A., ApJ, 1998, 503, 77
- Navarro J.F., Frenk C.S. & White S.D.M., 1995, MNRAS, 275, 720